Upper Layer Modification at Ocean Station *Papa*: Observations and Simulation[1]

K. L. DENMAN[2] AND M. MIYAKE

Institute of Oceanography, University of British Columbia, Vancouver 8, Canada

(Manuscript received 28 August 1972, in revised form 8 January 1973)

ABSTRACT

Time-series observations of the upper mixed layer of the ocean are presented for a six-week period at Ocean Station *Papa* in the northeast Pacific Ocean. These observations indicate the rate and extent of the wind-induced deepening of the mixed layer during the passage of several weather disturbances. The formation of the shallow layer of warm water that occurs under conditions of low winds and intense solar heating is also evident. A numerical model, developed by Denman, accurately predicts the behavior of the upper ocean during a 12-day period for which observed values of wind speed, solar radiation, and back radiation are used as input. To obtain realistic results, a value of 0.0012 for the ratio of the potential energy increase of the water column to the downward transfer rate of turbulent energy by the wind stress is used. This value is in agreement with that obtained from previous laboratory experiments (0.0015) indicating that the results obtained from such experiments are transferable to open ocean conditions.

1. Introduction

The annual growth and decay of the seasonal thermocline in the open ocean has been successfully explained by Kraus and Turner (1967; also Turner and Kraus, 1967) who modelled the annual cycle both theoretically and in the laboratory. Effects correlated with the passage of synoptic-scale weather systems (periods from 1–5 days) have not, however, been adequately investigated. Tully and Giovando (1963) described the formation and destruction of transient thermoclines by varying weather conditions, but their model was of a qualitative nature. Munk and Anderson (1948) presented an analysis of the influence of the fluxes of momentum, heat and moisture across the air-sea interface on the temperature and salinity structure in the upper ocean, but their treatment did not include any time dependence.

In this paper, data are presented which illustrate the behavior of the thermocline at Ocean Station *Papa* in the northeast Pacific Ocean during the passage of several synoptic-scale weather systems. The observed behavior is then simulated with a physical model of the upper ocean which requires only routine marine meteorological parameters as input (Denman, 1973). Finally, the observations are compared with the model output, and areas of discrepancy are discussed.

[1] A Bedford Institute of Oceanography contribution.

[2] Present affiliation: Fisheries Research Board of Canada, Marine Ecology Laboratory, Bedford Institute of Oceanography, Dartmouth, Nova Scotia, Canada.

2. Background data

Ocean Station *Papa* is a geographic position (50N, 145W) at which a Canadian weathership is continuously stationed. It is located in the eastern part of the subarctic Pacific region on the southern edge of the Arctic Gyre. According to Thomson (1971), typical geostrophic currents are in an east-northeast direction, roughly parallel to surface isotherms and isopycnals, with a speed of the order of 1 cm sec^{-1}. Wind-induced surface drift currents (see, for example, Lawford and Veley, 1956) and inertial currents (Defant, 1961) may be as large as 50 cm sec^{-1}, but as they are either transient or oscillatory they do not contribute appreciably to large-scale advection.

The influence of horizontal advection at Ocean Station *Papa* can be estimated from horizontal currents and temperature gradients. For typical surface temperature gradients in the northeast Pacific of about 1C $(100\ km)^{-1}$ and currents of 1–10 km day^{-1}, the maximum temperature change to be expected from advective effects would be about 1C in 10 days. From geostrophic transport calculations, Tabata (1965) attempted to estimate the temperature and salinity changes at *Papa* attributable to horizontal advection. He concluded that the average monthly temperature change at *Papa* due to advective effects for a five-year period was 0.26C $month^{-1}$, with a maximum of 0.78C $month^{-1}$. The average monthly salinity change was 0.02‰ $month^{-1}$, with a maximum of 0.05‰ $month^{-1}$. During the heating season, changes in sea surface temperature associated with synoptic-scale weather pat-

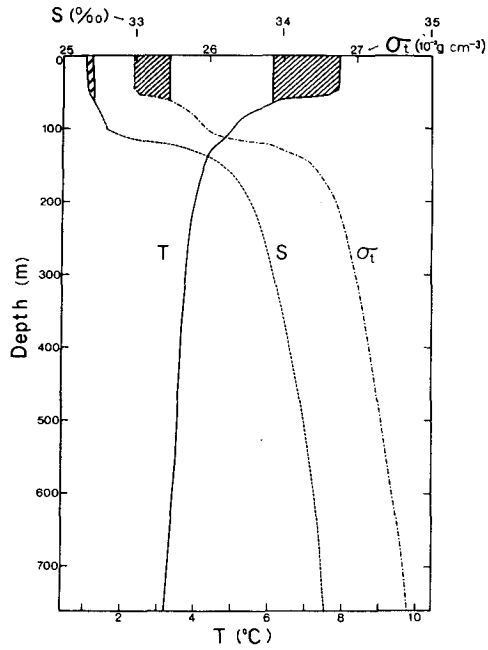

FIG. 1. An STD trace taken at Station *Papa* at 2100 GMT 23 June 1970. The hatched areas represent the change in T, S and σ_t that occurred since 19 May 1970.

terns are of the order of 1C over several days. This is at least an order of magnitude greater than changes expected from advective effects over the same time period. Therefore, one does not expect horizontal advection to affect significantly the heat budget of the upper layer of the ocean in the vicinity of *Papa* for periods less than several weeks.

Tabata (1961, 1965) and Thomson (1971) examined the vertical structure of the ocean at *Papa* in some detail. In any dynamic process in the ocean, it is the density structure, as determined by the temperature and salinity through the equation of state, which significantly influences the sequence of physical events. At *Papa* the main or permanent pycnocline occurs between 100 and 200 m: there, the salinity increases from 32.8 to 33.8‰, the temperature decreases from 4.5 to 4.0C, and σ_t increases from 26.0 to 26.8 (see Fig. 1). The density in this region is determined primarily by the salinity.

In summer, the seasonal thermocline forms in the upper 75 m: there, the temperature variations control the density variations. Typical summer variations in the upper layer as a result of synoptic-scale meteorological influences (lasting for 1–5 days) are $\Delta T = 2$C and $\Delta S = 0.06$‰. For mean values $T = 7$C and $S = 32.7$‰, the resulting variations in sigma t are $\Delta\sigma_t = -0.286$ and $+0.047$; the temperature effect is obviously larger. In the winter months, the salinity variations associated with the large evaporation at the sea surface may become significant.

The region of relatively small density change between the seasonal thermocline and the main pycnocline (i.e., over the depth range 50–100 m) in Fig. 1 was referred to as the "sub-thermocline duct" by Tully and Giovando (1963). As long as the seasonal thermocline is present, the sub-thermocline duct is sheltered from local meteorological effects. However, it is affected by horizontal advection and by entrainment from below. Because these processes vary from year to year, the sub-thermocline duct presents the upper mixed layer with a bottom boundary condition which also varies from year to year.

With increasing depth below the main pycnocline the gradients and curvatures of the temperature and salinity traces in Fig. 1 decrease. Below about 125 m, exponential curves could be fitted to the traces. The vertical structure in and below the main pycnocline is determined by the large-scale thermohaline circulation. An examination of the influence of the upper boundary conditions on the thermohaline circulation was carried out by Needler (1971).

From these previous studies, the following tentative conclusions can be drawn regarding the air-sea interaction at Ocean Station *Papa* during the summer months. First, the upper mixed layer is most stable from May to August, indicating that during the summer the mixing is essentially a wind-generated rather than a convective phenomenon. Second, the turbulent fluxes of heat are a minimum then, usually several times smaller than the back radiation, and we have ignored them. Third, because the rate of heating is greatest in the summer months, the temperature fluctuations in the upper layer associated with passing weather disturbances have the largest signal-to-noise ratio of any time during the year. Finally, the works of Tabata indicate that the advection of heat by ocean currents at *Papa* is not important for time scales much less than one month. The time of year best suited for a study of the wind mixing in the upper ocean at *Papa* was therefore determined to be the early summer months. We decided to carry out our program during a patrol of the Canadian weathership CCGS *Vancouver* at Ocean Station *Papa* in May and June, 1970.

3. Observational program

Routine oceanographic and meteorological observations have been taken every 3 hr at Ocean Station *Papa* for over 10 years. Although these observations have been used in previous studies of the upper ocean, more refined and more frequent measurements are required to delineate the physical processes involved in the time-dependent behavior of the mixed layer. The Canadian Meteorological Service (now Atmospheric Environment Service) agreed to make the routine observations immediately available during the cruise and arranged for the output from a wave gage to be recorded continuously for the duration of the cruise. The Canadian Marine Sciences Branch assisted in the program by providing expendable bathythermographs and a Bissett Berman

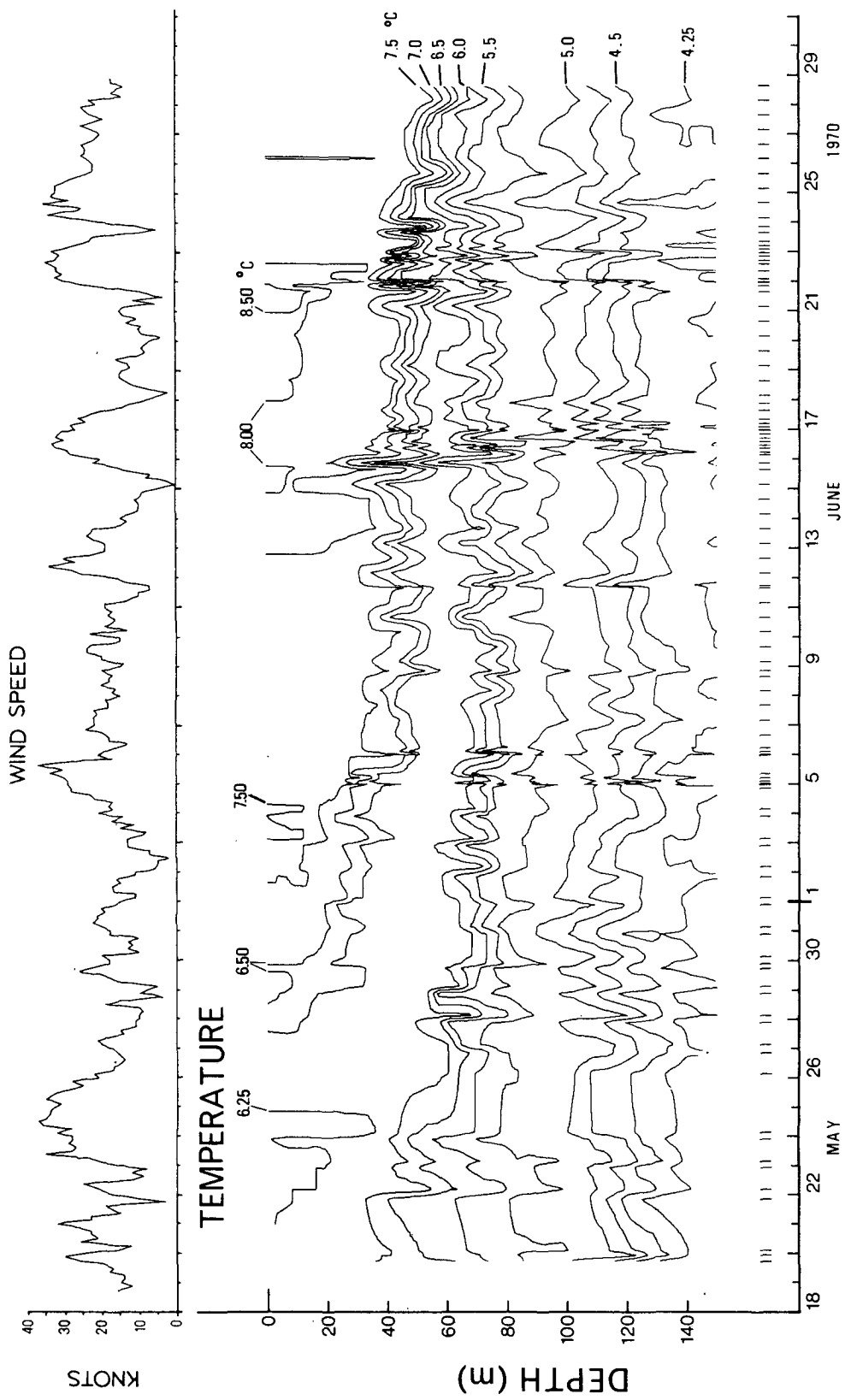

FIG. 2. Contours of constant temperature at Station *Papa* and 10 m wind speed for the period 19 May to 28 June, 1970. The temperature contours were obtained with a Bissett-Berman 9040 STD at the times marked by vertical bars just above the time axis.

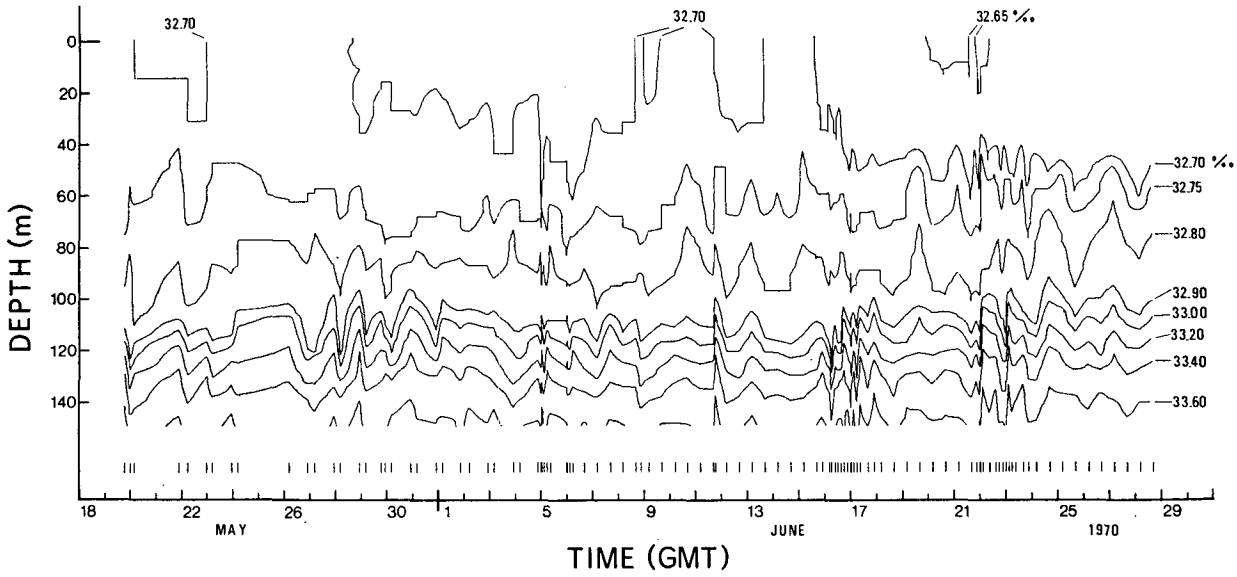

FIG. 3. Contours of constant salinity for the same period as in Fig. 2.

9040 STD so that hourly soundings of the upper ocean could be obtained during storms.

During the patrol at *Papa* during May and June 1970, a 6-week long series of STD (salinity-temperature-depth) profiles was obtained. The upper 150 m of the ocean was sampled eight times each day during storms and twice a day otherwise. Sippican XBT's (expendable bathythermographs) were also released at 1-hr intervals during storms. These series illustrate the time-dependent behavior of the seasonal thermocline as it was affected by intense summer heating and by the large variations in mean wind speed that accompanied several synoptic-scale weather disturbances.

a. Isopleth contours

The outputs from the STD observations to 150 m were digitized at 1 m intervals. Contours of isopleths of temperature and salinity were drawn in a depth vs time graph with a standard contouring program; these are shown in Figs. 2 and 3. The time of each observation is indicated by a vertical line immediately above the time axis. No smoothing has been done.

Notice, first, that in Fig. 2 the isotherms between 40 and 80 m converge with time during the period of high winds up to 25 May. At the end of this period, the upper mixed layer was essentially homogeneous in temperature down to 60 m, not unlike the upper layer during winter conditions. After 25 May, the seasonal thermocline started to form: shallow transient thermoclines built up during relatively calm periods only to be mixed down to about 45 m during each storm. This seasonal trend is relatively absent in the salinity contours in Fig. 3. The data plotted in Fig. 1 support this statement as can be seen from the hatched areas which represent changes near the surface from 19 May to 23 June, 1970. The salinity change affects sigma *t* only about one-eighth as much as does the change in temperature: the salinity, then, is apparently only passively involved in the development of the seasonal thermocline.

The frequency of sampling with the STD was greater during the three high wind periods: 5–6 June, 15–17 June, and 21–23 June. That the contours show much more structure during these periods is obvious; during the periods of twice daily sampling, higher frequency oscillations must have been present, but the slow rate of sampling did not resolve them. Even for the observations taken at 3-hr intervals, the apparent fluctuations in Figs. 2 and 3 are a direct result of the sampling rate. Fig. 4 illustrates the extent of the high-frequency motions for the storm period 22–23 June 1970. Isotherm contours were plotted from the hourly XBT profiles in exactly the same manner as from the STD profiles. Large-amplitude oscillations at the sampling frequency are evident in this plot only around 200 m depth; there, they result from the temperature change in 20 m being less than the temperature accuracy of the measurements. Near the seasonal thermocline, the dominant fluctuations occurred over periods of 8–9 hr. From 0000 to 1200 GMT on 22 June, the mixed layer thickened markedly and its temperature decreased as cooler water from below was entrained upward into the layer. The stratification at the bottom of the layer became more intense, as is indicated by the convergence of the isotherms between 20 and 60 m during the time up to 1200.

As the Brunt-Väisälä period at the bottom of the mixed layer was less than 10 min, effects resulting from unresolved internal waves with periods <1 hr must be

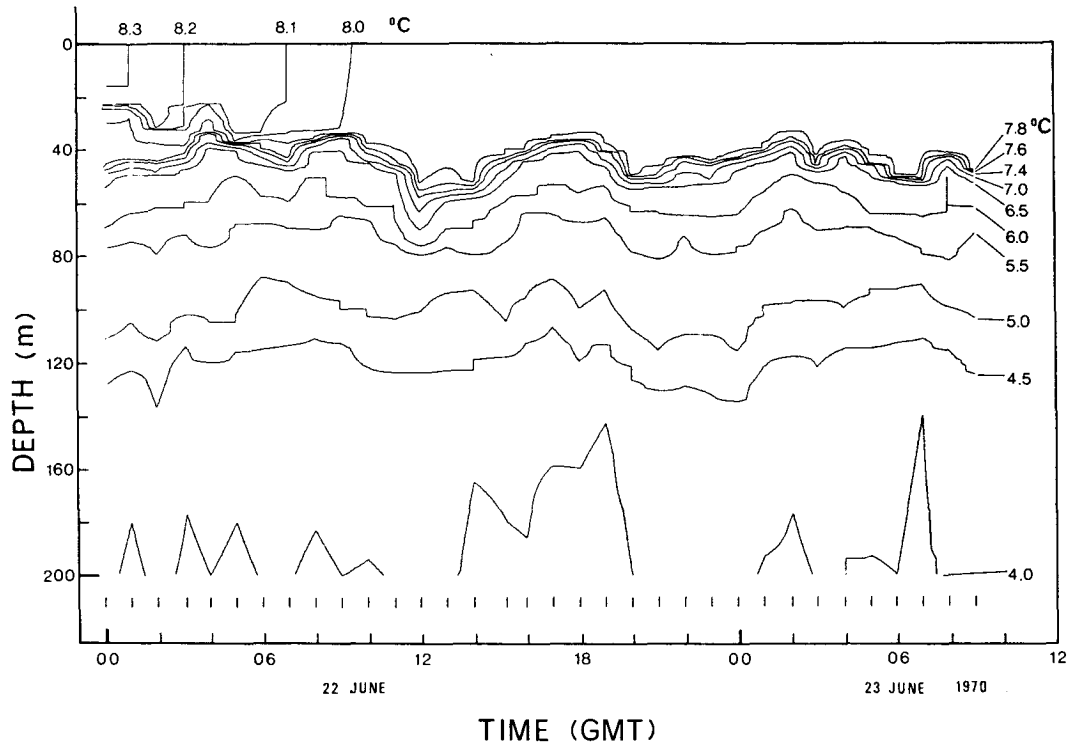

FIG. 4. Contours of constant temperature at Station *Papa* for the period 0000 GMT 22 June to 0900 GMT 23 June 1970. The traces were obtained hourly (as indicated by the vertical bars) with Sippican XBT's.

present in Fig. 4. However, the smoothness of the curves indicates that these were small compared to the fluctuations of 8–9 hr duration. We do not believe that these 8–9 hr fluctuations are "aliased" internal waves with periods <1 hr (see Blackman and Tukey, 1958) because for any given observation the ship was positioned randomly within a 10-km radius of 50N, 145W. The 6-week data series of Fig. 2 indicates that the seasonal trend and the changes occurring over several days that result from large-scale meteorological disturbances are easily distinguishable from the shorter period fluctuations.

b. Routine meteorological data

The corresponding routine meteorological data for the 6-week period of interest are plotted in Fig. 5. Note the seasonal trend evident in the sea surface temperature. The two bottom panels (wind speed and wave height) show a high degree of correlation on the synoptic meteorological scale (1–5 days). The period 13–25 June with its two well-defined weather systems will be examined in detail later.

4. Running the physical model

A model of the upper ocean was developed in Denman (1973) from the three equations for conservation of heat, mass and mechanical energy. The mixed layer in this model is a completely homogeneous layer bounded below by an arbitrary temperature gradient. The resulting equations describing the upper mixed layer are:

$$\frac{dT_s}{dt}=\frac{2}{h^2}[-(G-D)+h(B+H_e+H_s)+R(h-\gamma^{-1}+\gamma^{-1}e^{-\gamma h})], \tag{1}$$

$$H\left(w+\frac{dh}{dt}\right)=\frac{2[G-D+R\gamma^{-1}(1-e^{-\gamma h})]-h[B+H_e+H_s+R(1+e^{-\gamma h})]}{h(T_s-T_{-h})}, \tag{2}$$

$$dT_{-h}/dt=\gamma\,\mathrm{Re}^{-\gamma h}-(w+dh/dt)\partial T(-h)/\partial z. \tag{3}$$

In these equations, the time rates of change of the upper layer temperature (T_s) and thickness (h) are specified in terms of the turbulent energy derived from the wind stress ($G-D$), the net radiative heat input through the ocean surface ($R+B$), and the turbulent heat exchanges at the upper boundary (H_e+H_s). The

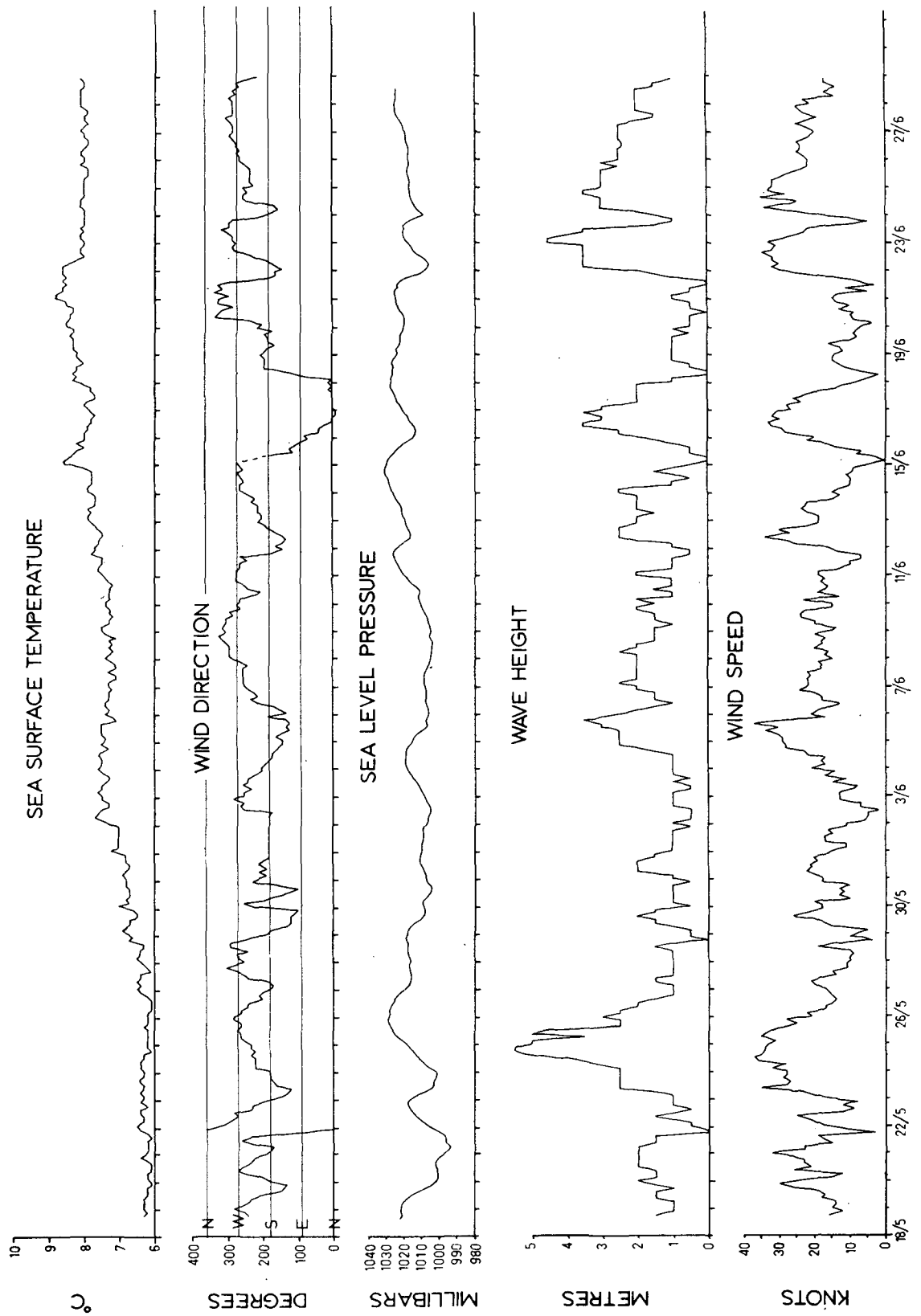

FIG. 5. Standard marine meteorological parameters measured every 3 hr at Station *Papa* by the Canadian Meteorological Branch for the period 18 May to 28 June, 1970.

vertical advective velocity imposed below the mixed layer is w, and H is the Heaviside step function having the properties:

$$H=\begin{cases}0, & \text{if } w+\dfrac{dh}{dt}\leqslant 0;\ \text{no entrainment mixing}\\ 1, & \text{if } w+\dfrac{dh}{dt}>0;\ \text{entrainment mixing at } z=h\end{cases}$$

As the temperature gradient below the layer, $\partial T(z)/\partial z$, varies with time because of solar heating and vertical advection, $\partial T(z)/\partial z$ must be known at any time t in order to evaluate $\partial T(-h)/\partial z$ in (3). The necessary boundary condition is

$$\partial T(z)/\partial t=\gamma\,\mathrm{Re}^{\gamma z}-w\partial T(z)/\partial z,\quad z\leqslant -h. \qquad (4)$$

The two adjustable parameters are γ, the extinction coefficient of the solar radiation, and m, the fraction of the wind stress energy at 10 m height which is eventually used to increase the potential energy of the water column (to be defined later).

a. The extinction coefficient

Solar radiation incident on the sea surface is confined to the visible and infrared regions: the spectrum is composed of wavelengths ranging from 0.3–1.0 μm (Jerlov, 1968). For wavelengths >1.0 μm, most of the radiation is absorbed within the upper few centimeters of the ocean. Much of this absorbed heat is reradiated back to the atmosphere. For wavelengths between 0.3 and 1.0 μm, the radiation penetrates to much greater depths. Although the absorption within this band varies with wavelength, an average extinction coefficient γ (cm^{-1}) for wavelengths from 0.3–1.0 μm can be defined such that the rate of solar heating at some depth $z=-d$ can be expressed as $R(-d)=R(0)e^{-\gamma d}$. The ocean also acts as an approximate blackbody radiator. The resulting back radiation to the atmosphere, $-B$, is assumed to occur at the surface within a layer of water of negligible thickness.

b. Energy available for mixing

Most of the momentum transported into the ocean by the wind stress is used to generate surface waves (Dobson, 1971). Some of this wave energy is advected away, some is dissipated or transformed into turbulence through wave breaking in the upper few meters, and some is transferred into a drift current. The breaking waves and vertical shear of this drift current provide sources for turbulent energy production on small scales. The turbulent energy may be dissipated, it may be used to increase the potential energy of the water column by doing work against the buoyancy forces, or it may be used to increase the kinetic energy of the mean flow. Turner (1969) suggested that the rate of increase in potential energy of the upper ocean as a result of work done by mixing is approximately a constant fraction m of the rate of turbulent energy transferred downward by the wind stress at 10 m above the surface. If $G_*-D_*[=\rho_0\alpha g(G-D)$, where α is the coefficient of thermal expansion] is the rate at which wind stress energy is made available for mixing within the upper layer, then

$$m=(G_*-D_*)/(\tau\langle U_{10}\rangle)=(G_*-D_*)/(\rho_a C_{10}\langle U_{10}\rangle^3), \qquad (5)$$

where ρ_a and ρ_0 are average air and water densities and τ is the wind stress.

Implicit in any assumptions about m is also some assumption concerning the drag coefficient C_{10}. Measurements indicate that C_{10} does not vary appreciably for mean wind speeds up to at least 18 m sec^{-1} (Denman and Miyake, 1973). Eq. (5) shows that if C_{10} is constant, then the parameterization of the energy available for mixing involves only one adjustable constant, m.

5. Results

In this section, data for the 6-week cruise period are examined to determine appropriate values of the two adjustable parameters. For these parameter values, the numerical model is run with real input data consisting of hourly values of wind speed, solar radiation, and back radiation from the sea surface. One period of 12 days and one 2-day storm period are examined.

a. The input data

Physically realistic values for the adjustable parameters are necessary input for the model. One of the adjustable parameters is m, the ratio of potential energy change to the rate of production of wind stress energy. A value of $m=0.0012$ gave realistic results in the idealized studies of wind mixing and diurnal heating discussed in Denman (1973). From the results of Kato and Phillips (1969), who carried out a mixing experiment in the laboratory, one can calculate a value for m of 0.0015. These are both considerably smaller than the value 0.01 obtained by Turner (1969) for some actual field data.

The other adjustable parameter in the model is γ, the extinction coefficient of solar radiation in sea water. From Jerlov (1968), a reasonable range for the extinction coefficient in open ocean waters found at Ocean Station *Papa* is 0.001–0.003 cm^{-1}. Parsons *et al.* (1966) used photometer measurements obtained at *Papa* (see also McAllister *et al.*, 1959, and Parsons and Anderson, 1970) to calibrate the Secchi disk readings. They estimated the extinction coefficient γ to be in the range 0.001–0.002 cm^{-1} at *Papa* during May and June. The value of $\gamma=0.002$ cm^{-1} used in the diurnal model discussed in the preceding paper is within the ranges just presented.

The oceanographic observations described in the previous sections indicate that none of the sensible and

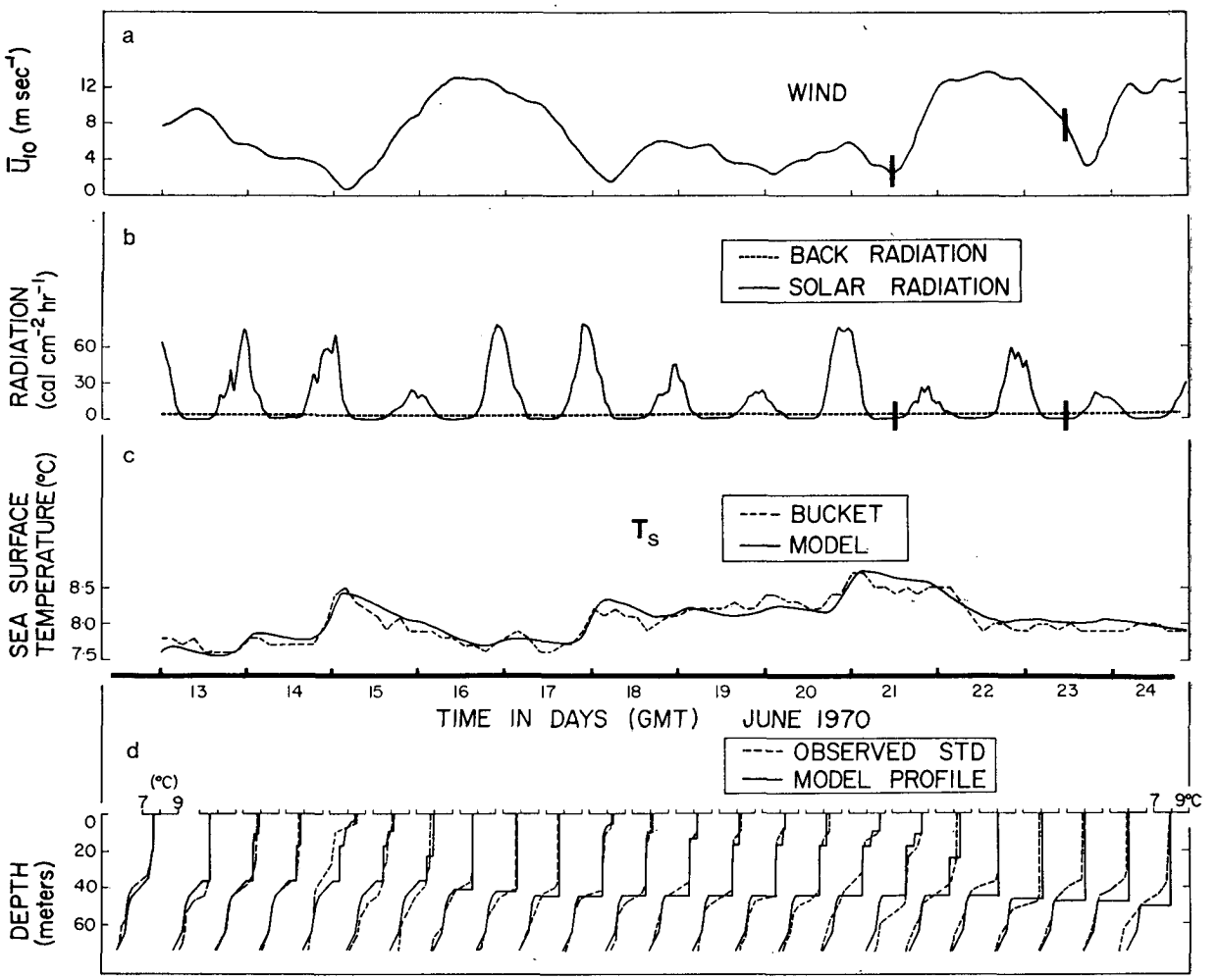

FIG. 6. Input and results of the model (Run 3) for the period 13–24 June 1970: (a) and (b) are the observed data inputs to the model: $\bar{U}_{10}$ is the mean wind estimated from the 3-hr observations from cup anemometers, and R and $-B$ are the measured incident solar radiation and calculated back radiation at the sea surface; (c) is the comparison of the predicted sea surface temperature with that observed from bucket measurements; and (d) is the comparison of the temperature profiles of the model (each 12 hr) with those obtained with an STD (where available). The parameter values were $m=0.0012$ and $\gamma=0.003$ cm^{-1}. See legend to Fig. 7.

latent heat fluxes across the air-sea interface, the horizontal advection of heat by ocean currents, and the vertical advection from below the layer are important to the heat balance of the upper mixed layer during the summer months.

If the turbulent and advective heat fluxes are ignored, then the boundary conditions are derived from hourly values of solar radiation R_*, back radiation $-B_*$, and wind speed at 10 m $\langle U_{10}\rangle$. The hourly values of solar radiation are those obtained from the pyranometer output (Canadian Monthly Radiation Summary, 1970). The routine estimates of wind speed taken every 3 hr were smoothed and interpolated to 1-hr intervals. The estimates of back radiation for 12-hr periods, which were calculated using empirical formulas of Laevastu (1960, 1963), were also interpolated and smoothed to give hourly values. The boundary conditions, $\langle U_{10}\rangle$, R_* and B_*, are shown in the upper two panels of Fig. 6. The initial temperature profile is also shown at the bottom left of the figure; it was estimated from the STD profiles taken near 0000 GMT 13 June.

b. The 12-day period

The results of the model calculations for the 12-day period, 13–24 June 1970, are presented here. The values of the parameters m and γ were progressively adjusted for Runs 1, 2 and 3 as described below. Only the results for Run 3 are plotted. In Run 1 ($m=0.0025$, $\gamma=0.002$ cm^{-1}), the mixed layer thickness calculated by the model slowly departed from the observed mixed layer thickness until, on the twelfth day, it exceeded 75 m. At that time, the observed thickness of the mixed layer was only about 50 m.

In Run 2 ($m=0.0012$, $\gamma=0.002$ cm^{-1}), setting $m=0.0012$ was equivalent to using the friction velocity in the water, $w_*=(\tau/\rho_0)^{\frac{1}{2}}$, as the scaling velocity in G_*,

the energy available for mixing. The computed behavior of the mixed layer during the stormy periods reproduced quite closely the observed behavior. During the heating periods, however, the layer depth was about 60% too large, and the sea surface temperature did not reach the pronounced peaks present in the real data. From the theoretical results (Denman, 1973) we know that in the model the thickness of the mixed layer during low winds had been decreased significantly by increasing the extinction coefficient. The extinction coefficient was therefore increased from 0.002 to 0.003 cm^{-1} in the next run.

For Run 3 ($m=0.0012$, $\gamma=0.003$ cm^{-1}), the resulting sea surface temperature and twice-daily temperature profiles calculated from the model are plotted in Fig. 6. The observed temperature profiles superimposed on the model profiles were obtained, in all cases, within 1 hr of the time for which they are plotted.

The agreement between the predicted and observed sea surface temperature is very good on time scales greater than one day. The model profiles, while obviously idealized, do reproduce the time-dependent behavior of the mixed layer. Deepening of the mixed layer resulting from the high winds during the periods 15–17 and 21–23 June is simulated satisfactorily. The shallow warm layer which built up during 14–15 June and again during 18–21 June is also evident in the model profiles. The general agreement indicates that the model representation of the time-dependent behavior of the upper mixed layer is quite good.

The observed sea surface temperature, represented by the dashed line in Fig. 6, was obtained from standard bucket temperatures taken every 3 hr; the measurement error in these data is $\pm(0.05-0.10)$C. That bucket measurements do not accurately determine the surface "skin" temperature (resulting from back radiation) is not important here because the model does not predict the skin temperature either, but rather the average mixed layer temperature.

Because the boundary inputs to the model were smoothed somewhat, fluctuations in the observed sea surface temperature that occurred in less than $\sim$12 hr are not predicted by the model. Such fluctuations probably result from the frequency and accuracy of the sampling technique and can thus be neglected. On the other hand, the larger variations in sea surface temperature on scales of 2–3 days are associated with the synoptic meteorological inputs, and are accurately reproduced by the model to within 0.1C.

One can observe a diurnal variation in the model estimate of the sea surface temperature. However, any such variation in the observations is obscured by measurement errors; thus, it might be recovered by a Fourier analysis of observed summer sea surface temperatures.

c. A 2-day storm period

The model was also run with the same parameter values used in Run 3 for the 48-hr storm period 21–23 June denoted by the vertical bars in Fig. 6. During this storm, STD profiles were taken every 3 hr, and XBT profiles were taken every hour in order that the rate of deepening of the mixed layer as well as its eventual depth of penetration might be determined.

The results of the model calculations are plotted in Fig. 7. Surface temperature measurements from the STD traces, from the XBT traces and from bucket values, and the surface temperatures calculated using the model are plotted in Fig. 7a. Fig. 7b shows observed and computed estimates of the mixed layer depth. The error bars represent the observed depth range of strongest stratification just below the layer. From the XBT profiles, a point estimate of the mixed layer depth has been plotted; the error in this estimate is about ±5 m. At the bottom of Fig. 7, the available STD profiles have been superimposed on temperature profiles computed from the model at 3-hr intervals.

The sea surface temperatures estimated by the model agree with the STD and XBT values within the uncertainty of the measurements; bucket temperatures, as one might expect, show less consistency. The model predicts correctly the mean rate of deepening within the accuracy to which it can be determined from the observations; the scatter in the observed mixed layer depth is mostly attributable to internal waves.

6. Possible sources of discrepancy

With actual meteorological inputs and adjustable constants, the model reproduces the observed time-dependent behavior of the upper mixed layer. The sea surface temperature derived from the model is consistent with the actual observations within the limits of the errors in measurement. However, the depth and shape of the simulated mixed layer do show some differences from the depth and shape of the observed mixed layer. A discussion of the possible sources of the discrepancies between the model and the observations is presented in this section.

a. Currents in the mixed layer

Hasselmann (1970) described a possible sequence of responses of the upper mixed layer of the ocean to the passage of a synoptic weather disturbance. The responses to meteorological forcing which lasts only a few hours are transient and highly time dependent. For forcing which lasts about one-quarter to one-half an inertial period (15.7 hr at 50° latitude), the response will very likely include inertial oscillations (Ekman, 1905; Gustafson and Kullenberg, 1936). For forcing which lasts considerably longer than one day, Ekman transports are set up in the upper layer with large-scale divergences and convergences resulting from non-zero

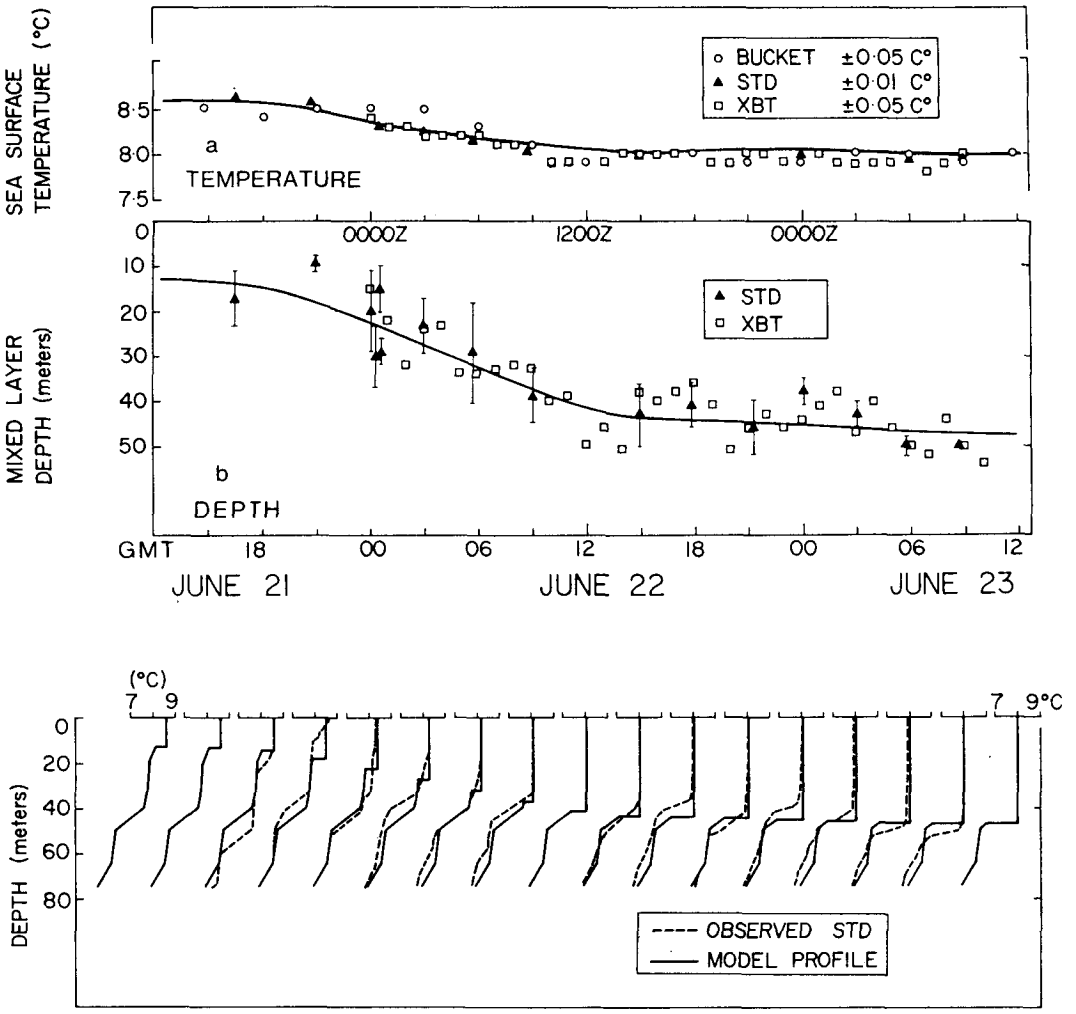

FIG. 7. Comparison of the model output with the observed data for the storm period 1200 GMT 21 June to 1200 GMT 23 June, 1970. The inputs were just those in Fig. 6 for the period denoted by heavy vertical bars. The parameter values were $m=0.0012$ and $\gamma=0.003$ cm^{-1}. The error bars in (b) for the mixed layer depth from the STD profiles represent the observed depth range of strongest stratification immediately below the layer. The error in the XBT estimates of mixed layer depth is $\sim\pm 5$ m.

curl in the surface wind stress field (Fofonoff, 1962; Roden, 1969).

The generation of inertial period currents by moving storm patterns was investigated by Pollard (1970), and Pollard and Millard (1970). For such forcing, the upper mixed layer appears to respond like a slab: the influence on the vertical structure of temperature and salinity at a single point would be expected to be small relative to the effects due to local wind mixing. The observations presented here substantiate this reasoning.

b. Turbulent and advective heat fluxes

The agreement of the model with the observed data seems to justify neglecting both the transfer of heat from the air-sea interface by turbulent processes and the advection of heat by horizontal ocean currents. In a study such as this one, the advection of heat by horizontal ocean currents for times less than one month can probably be neglected during any season. However, the sensible and latent heat fluxes could possibly account for some of the variation between the model results and the observations. We estimated these heat fluxes from the routine meteorological data using the aerodynamic formulas of Jacobs (1951) with the exchange coefficients determined by Pond *et al.* (1971). Calculations every 12 hr for the period 13–25 June 1970 gave a mean heat loss at the sea surface due to the turbulent fluxes of heat and moisture of roughly -25 to -30 cal cm^{-2} day^{-1} which was about one-third of the average back radiation. On two occasions the heat loss due to the turbulent fluxes was the same size as the back radiation; neglecting the turbulent heat fluxes during the buildup of the summer thermocline probably causes appreciable errors only on isolated occasions.

c. Internal waves

Many of the variations in the depth of the mixed layer and in the shape of the temperature profile below the mixed layer can be attributed to internal waves which have periods ranging from the Brunt-Väisälä period, of about 1–10 min in the upper ocean, to the local inertial period of 15.7 hr (at latitude 50°). The shorter period waves, which may be excited by either tidal or indirect meteorological forcing, have characteristic wavelengths of the order of hundreds of meters or of kilometers (see, e.g., LaFond, 1964). These internal waves, with their inherent convergences and divergences, are responsible for much of the point-to-point variation in the mixed layer depth plotted in Fig. 7. However, the effects coupled to the moving storm systems are easily discernible in the data presented.

d. Turbulent dissipation

Dissipation of energy within the upper mixed layer has been included implicitly in the formulation of m, the fraction of the downward transfer of energy by the wind stress 10 m above the sea surface, used to increase the potential energy of the water column by mixing. However, if the model is to be applicable over wide ranges of wind speeds and surface heat losses, the dissipation should be treated explicitly. Before a more complicated assumption about the effect of the dissipation on the mixing energy is incorporated into a model such as this, more experiments on the mechanisms of energy partition in the upper layer of the ocean must be carried out.

7. Conclusions

Observations have been obtained from Ocean Station *Papa* which illustrate the behavior of the upper mixed layer during the passage of several synoptic meteorological disturbances. This time series allows a quantitative determination of the rate and extent of the wind-driven deepening of the oceanic mixed layer.

A physical model of the upper mixed layer (Denman, 1973) was used to predict the variations in the temperature structure evident in the time series measurements. The model accurately simulated the behavior of the upper mixed layer at *Papa* over a 12-day period; the data used as input to the model were the observed values of wind speed, solar radiation, and back radiation. The ratio, $m=0.0012$, of the energy available for mixing to that transferred downward by the wind at 10 m, needed for the model to yield results consistent with the real profiles, agrees with the value ($m=0.0015$) calculated from the laboratory experiments of Kato and Phillips (1969). The radiation extinction coefficient used in the model is shown to be consistent with values observed by other authors. Other heat transfer mechanisms such as latent and sensible heat fluxes at the ocean surface, and horizontal or vertical advection within the ocean itself appear not to be important to the spring development of the summer thermocline at Station *Papa*.

The good agreement of the model simulation with the observations indicates that on time scales of 1–5 days the local responses to the meteorological forcing dominate both the internal waves and the large-scale responses. To study the horizontal gradients of these large-scale effects, one must extend this model to a horizontal grid and to longer time scales. That would require extensive knowledge (which is not available at the present time) of the temporal and spatial behavior of the temperature and salinity gradients at the bottom of the well-mixed layer.

Acknowledgments. The authors would like to thank the officers and crew of the Canadian weathership C.C.G.S. *Vancouver* for their help and cooperation during the data collection. Special thanks go to Mr. Bernard Minkley (Marine Sciences Branch) and Mr. Ron Johnson (University of British Columbia) who assisted during the seven week cruise to Station *Papa*. We would like to acknowledge the various Canadian Government agencies who supported this research financially. The Marine Sciences Branch and the Meteorological Branch made equipment, data and personnel available for this study. The U. S. Office of Naval Research also provided funds and the National Research Council of Canada supported K. Denman personally. Finally, we would like to thank Drs. R. W. Burling and R. W. Stewart for their many helpful comments.

REFERENCES

Blackman, R. B., and J. W. Tukey, 1958: *The Measurement of Power Spectra*. New York, Dover, p. 31.

Canadian Monthly Radiation Summary, 1970: Meteorological Branch, Department of Transport.

Defant, Albert, 1961: *Physical Oceanography*, Vol. 1. New York, Pergamon, p. 443.

Denman, K. L., 1973: A time-dependent model of the upper ocean. *J. Phys. Oceanogr.*, **3**, 173–184.

——, and M. Miyake, 1973: The behavior of the mean wind, the drag coefficient, and the wave field in the open ocean. *J. Geophys. Res.* (in press).

Dobson, Frederic William, 1971: Measurements of atmospheric pressure on wind-generated sea waves. *J. Fluid Mech.*, **48**, 91–127.

Ekman, V. W., 1905: On the influence of the earth's rotation on ocean currents. *Ark. Mat. Astron. Fys.*, **2**, No. 11.

Fofonoff, N. P., 1962: Machine computations of mass transport in the North Pacific Ocean. *J. Fish. Res. Bd. Can.*, **19**, 1121–1141.

Gustafson, T., and B. Kullenberg, 1936: Untersuchungen von Trägheitsströmungen in der Ostsee. *Sv. Hydr.-Biol. Komm. Skr. Ny., Ser. Hydr.*, No. 13.

Hasselmann, K., 1970: Wave-driven inertial oscillations. *Geophys. Fluid Dyn.*, **1**, 463–502.

Jacobs, W. C., 1951: Large-scale aspects of energy transformation over the oceans. *Compendium of Meteorology*, Boston, Amer. Meteor. Soc., 1057–1070.

Jerlov, N. G., 1968: *Optical Oceanography*. London, Elsevier, 199 pp.

Kato, H., and O. M. Phillips, 1969: On the penetration of a turbulent layer into a stratified fluid, *J. Fluid Mech.*, **37**, 643–655.

Kraus, E. B., and J. S. Turner, 1967: A one-dimensional model of the seasonal thermocline. II, The general theory and its consequences. *Tellus*, **19**, 98–106.

Laevastu, T., 1960: Factors affecting the temperature of the surface layer of the sea. *Commentat. Phys.-Math.*, **25**, 1–136.

——, 1963: Energy exchange in the North Pacific. Part I, Formulas and nomographs. Rept. 29, Hawaii Institute of Geophysics.

LaFond, E. C., 1964: Three-dimensional measurements of sea temperature structure. *Studies on Oceanography*, University of Washington Press, 314–320.

Lawford, A. L., and V. F. C. Veley, 1956: Change in the relationship between wind and surface water movements at higher wind speeds, *Trans. Amer. Geophys. Union*, **6**, 691–693.

McAllister, C. D., T. R. Parsons and J. D. H. Strickland, 1959: Data record oceanic fertility and productivity measurements at Ocean Weather Station "P" July and August 1959. *Fish. Res. Bd. Can., Ms. Rept. Ser.*, No. 55.

Munk, W. H., and E. R. Anderson, 1948: Notes on a theory of the thermocline. *J. Marine Res.*, **7**, 276–295.

Needler, G. T., 1971: Thermocline models with arbitrary barotropic flow. *Deep-Sea Res.*, **18**, 895–903.

Parsons, T. R., and G. C. Anderson, 1970: Large-scale studies of primary production in the North Pacific Ocean. *Deep-Sea Res.*, **17**, 765–776.

——, L. F. Giovando and R. J. LeBrasseur, 1966: The advent of the spring bloom in the eastern subarctic Pacific Ocean. *J. Fish. Res. Can.*, **23**, 539–546.

Pollard, R. T., 1970: On the generation by winds of inertial waves in the ocean. *Deep-Sea Res.*, **17**, 795–812.

——, and R. C. Millard, Jr., 1970: Comparison between observed and simulated wind-generated inertial oscillations. *Deep-Sea Res.*, **17**, 813–821.

Pond, S., G. T. Phelps, J. E. Paquin, G. McBean and R. W. Stewart, 1971: Measurements of the turbulent fluxes of momentum, moisture and sensible heat over the ocean. *J. Atmos. Sci.*, **28**, 901–917.

Roden, G. I., 1969: Winter circulation in the Gulf of Alaska. *J. Geophys. Res.*, **74**, 4523–4534.

Tabata, Susumu, 1961: Temporal changes of salinity, temperature, and dissolved oxygen content of the water at Station "P" in the northeast Pacific Ocean, and some of their determining factors. *J. Fish. Res. Bd. Can.*, **18**, 1073–1124.

——, 1965: Variability of oceanographic conditions at Ocean Station "P" in the northeast Pacific Ocean. *Trans. Roy. Soc. Can., Ser. 4*, **3**, Section 3, 367–418.

Thomson, Richard Edward, 1971: Theoretical studies of the circulation of the subarctic Pacific region and the generation of Kelvin type waves by atmospheric disturbances. Ph.D. thesis, Institute of Oceanography, University of British Columbia.

Tully, J. P., and L. F. Giovando, 1963: Seasonal temperature structure in the eastern subarctic Pacific Ocean. *Roy. Soc. Canada, Spec. Publ.*, No. 5 (M. J. Dunbar, Ed.), 10–36.

Turner, J. S., 1969: A note on wind mixing at the seasonal thermocline. *Deep-Sea Res.*, **16** Suppl. 297–300.

——, and E. B. Kraus (1967), A one-dimensional model of the seasonal thermocline. I, A laboratory experiment and its interpretation. *Tellus*, **19**, 88–97.